



Article

N-Heterocyclic Carbene–Palladium Functionalized Coordination Polymer (Pd-NHC@Eu-BCI) as an Efficient Heterogeneous Catalyst in the Suzuki–Miyaura Coupling Reaction

Lixin You ¹, Rui Tan ¹, Xiaojuan Wang ¹, Jianhong Hao ¹, Shiyu Xie ¹, Gang Xiong ¹, Fu Ding ^{1,2}, Andrei S. Potapov ^{3,*} and Yaguang Sun ^{1,2,*}

- ¹ Key Laboratory of Inorganic Molecule-Based Chemistry of Liaoning Province, Shenyang University of Chemical Technology, Shenyang 110142, China
- ² Key Laboratory on Resources Chemicals and Material of Ministry of Education, Shenyang University of Chemical Technology, Shenyang 110142, China
- ³ Nikolaev Institute of Inorganic Chemistry, Siberian Branch of the Russian Academy of Sciences, Lavrentiev Ave., 3, 630090 Novosibirsk, Russia
- * Correspondence: potapov@niic.nsc.ru (A.S.P.); sunyaguang@syuct.edu.cn (Y.S.)

Abstract: In the present work, a new heterogeneous catalyst Pd-NHC@Eu-BCI was synthesized by introducing N-heterocyclic carbene–palladium active sites into a 2D coordination polymer [Eu(BCI)(NO₃)₂H₂O]_n (Eu-BCI) based on a 1,3-bis(carboxymethyl)imidazolium (HBCI) ligand. The catalyst was characterized by various analytical techniques such as X-ray photoelectron spectroscopy (XPS), inductively coupled plasma atomic emission spectroscopy (ICP-AES), energy-dispersive X-ray spectroscopy (EDS), scanning electron microscopy (SEM), transmission electron microscopy (TEM), powder X-ray diffraction (PXRD), infrared spectroscopy (IR) and thermogravimetric analysis (TGA). Catalytic activity of Pd-NHC@Eu-BCI was tested for the Suzuki–Miyaura cross-coupling reaction. The catalyst from the reaction mixture was easily recovered by filtration and still exhibited good catalytic activity and maintained its original structure after five cycles.

Keywords: N-heterocyclic carbene–palladium; coordination polymer; heterogeneous catalyst; Suzuki–Miyaura reaction



Citation: You, L.; Tan, R.; Wang, X.; Hao, J.; Xie, S.; Xiong, G.; Ding, F.; Potapov, A.S.; Sun, Y. N-Heterocyclic Carbene–Palladium Functionalized Coordination Polymer (Pd-NHC@Eu-BCI) as an Efficient Heterogeneous Catalyst in the Suzuki–Miyaura Coupling Reaction. *Crystals* **2023**, *13*, 341. <https://doi.org/10.3390/cryst13020341>

Academic Editor: Kil Sik Min

Received: 19 December 2022

Revised: 13 January 2023

Accepted: 3 February 2023

Published: 17 February 2023



Copyright: © 2023 by the authors. Licensee MDPI, Basel, Switzerland. This article is an open access article distributed under the terms and conditions of the Creative Commons Attribution (CC BY) license (<https://creativecommons.org/licenses/by/4.0/>).

1. Introduction

Palladium-containing coordination polymers, used in the C–C cross-coupling reactions, have been intensively explored owing to their versatile protocol for useful reaction products and important role in industrial processes [1–11]. N-heterocyclic carbene (NHC)–metal complexes possessing strong metal–carbene bonds open up a new way in organometallic catalysis [12–14], and have been applied to speed up various organic reactions, such as C–N bond formation [15,16], cycloaddition of CO₂ to epoxides [17,18], olefin metathesis [19,20], hydrogenation [21] and C–C cross-coupling reactions [22,23]. In particular, the use of transition-metal-catalyzed cross-coupling reactions for the formation of biaryl C–C bonds is attracting significant attention. The N-heterocyclic carbene–palladium (NHC–Pd) complexes, including PEPPSI–Pd–NHC [24,25], CNC-type Pd pincer [26,27], Pd(IPr)₂Cl [28], palladium–NHC–pyridine [29] and Pd–NHC–MOF [30], showed excellent activities in the Suzuki–Miyaura reactions. Nevertheless, the most important disadvantage of homogeneous catalysts is that they are not recyclable and can contaminate the reaction products [31]. In this case, the organometallic catalyst fixed in a filterable support is a suitable method to prevent metal contamination of the products [32]. Many supported catalysts have been prepared, but only a few examples are used in industrial applications [33,34]. To overcome the problematic issues in the homogeneous phase, the heterogeneous catalysts with all

homogeneous catalyst features, such as efficiency, reproducible synthesis and easy and full chemical characterization, are still of concern to chemists [35,36].

The NHC-Pd functionalized coordination polymers (CPs) can easily be realized by the post-synthetic modification (PSM) of a stable CP containing the imidazolium ligand; Here we assumed a two-step method to construct a new heterogeneous catalyst, which makes the palladium-containing catalyst recoverable and reusable [37,38]. Therefore, in continuing our previous works [1,39–44], we report herein the synthesis, characterization and catalytic activity of the Pd-NHC@Eu-BCI, which was a NHC-Pd functionalized Eu-BCI {Eu-BCI = [Eu(BCI)(NO₃)₂H₂O]_n} based on a 1,3-bis(carboxymethyl) imidazolium (HBCI) ligand. The catalyst has good stability and shows excellent catalytic performance and recyclability in the Suzuki–Miyaura cross-coupling reaction.

2. Materials and Methods

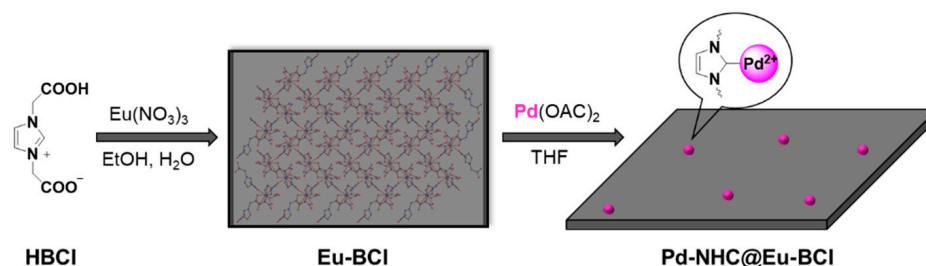
All chemicals were purchased from commercial sources and were used without further purification.

2.1. Synthesis of Eu-BCI

Eu-BCI was synthesized according to a previous report [45]. HBCI (0.2 mmol) and Eu(NO₃)₃ (0.1 mmol) were added to a 23 mL Teflon-lined autoclave with a mixture of ethanol and H₂O. The reaction mixture was kept at 110 °C for three days. The product was obtained and washed with absolute ethanol.

2.2. Synthesis of Pd-NHC@Eu-BCI

Eu-BCI (0.54 g, 1.0 mmol) and Pd(OAc)₂ (0.314 g, 1.4 mmol) were stirred in 100 mL tetrahydrofuran (THF) solution for 12 h under an argon atmosphere. Then the reaction mixture was heated to 70 °C and refluxed for 24 h under an argon atmosphere. Light grey powder was collected by filtration, washed with THF (3 × 5 mL), MeOH (2 × 5 mL) and Et₂O (2 × 5 mL), and dried in vacuum (Scheme 1). The ICP-AES measurement of Pd-NHC@Eu-BCI indicated that the palladium content was 1.15 wt. %.



Scheme 1. Synthesis route of Pd-NHC@Eu-BCI.

2.3. Characterization

Powder X-ray diffraction (PXRD) was performed with a Rigaku smartLab 9k diffractometer. Infrared spectroscopy (IR) spectra were recorded on a Nicolet IR-470 spectrometer using KBr pellets. Thermogravimetric analyses (TGA) were carried out on a NETZSCH STA449F5 instrument under Ar gas flow at a uniform heating rate of 10 °C min⁻¹ in the range of 27–800 °C. Scanning electron microscopy (SEM) was performed on Quanta FEG450. X-ray photoelectron spectroscopy (XPS) measurements were performed on an ESCALAB250 X-ray photoelectron spectroscopy, using Mg K α X-ray as the excitation source. Inductively coupled plasma atomic emission spectroscopy (ICP-AES) was completed on Thermo IRIS Advantage. ¹H NMR spectra were recorded on a Bruker BioSpin GmbH AVANCE III 500 MHz spectrometer. Gas chromatography (GC) analyses were performed on an Agilent Technologies 7890A gas chromatograph.

2.4. Catalytic Activity Tests

Aryl halide (1.0 mmol), phenylboronic acid (1.2 mmol), base (2.0 mmol) and Pd-NHC@Eu-BCI were added to a 35 mL Schlenk tube. Then 5.0 mL of solvent was added, and the mixture was stirred in air at the appropriate temperature for the certain time. The solution obtained after the reaction was extracted with ethyl acetate (20 mL). The product yield was determined by GC analysis using hexadecane as the internal standard. The catalyst was separated by centrifugation, and finally washed with absolute ethanol, dried under vacuum and then used in the next catalytic experiment.

3. Results and Discussions

3.1. Catalyst Characterization

Infrared spectroscopy (IR) spectra of Eu-BCI and Pd-NHC@Eu-BCI are shown in Figures S1 and S2. The Eu-BCI showed an absorption peak around 3352 cm^{-1} , which was attributed to the O–H stretching vibration of the coordinated water. The absorption peaks at 3159 cm^{-1} , 3111 cm^{-1} , 1654 cm^{-1} and 1416 cm^{-1} were assigned to characteristic peaks of the imidazolium ring. The asymmetric and symmetric stretching vibrations of the carboxylate, found at 1589 cm^{-1} and 1311 cm^{-1} , indicate that the HBCI ligands were completely deprotonated when coordinating to the Eu ions. The Pd-NHC@Eu-BCI showed a similar pattern with Eu-BCI, indicating the structure was maintained after PSM.

The 2D Eu-BCI was synthesized according to the method in the literature (Figure S3) [45]. Powder X-ray diffraction (PXRD) was used to confirm the phase purity of the crystalline framework and the resulting diffractograms are presented in Figure 1. A good phase purity and homogeneity of the Eu-BCI was confirmed since the PXRD patterns are in good agreement with the calculated ones obtained from the single-crystal structure data. Furthermore, the skeleton was maintained after PSM, as shown in the same PXRD patterns of the synthesized Eu-BCI and Pd-NHC@Eu-BCI. Therefore, the structure of the synthesized Eu-BCI can tolerate such modified conditions without the collapse of the framework.

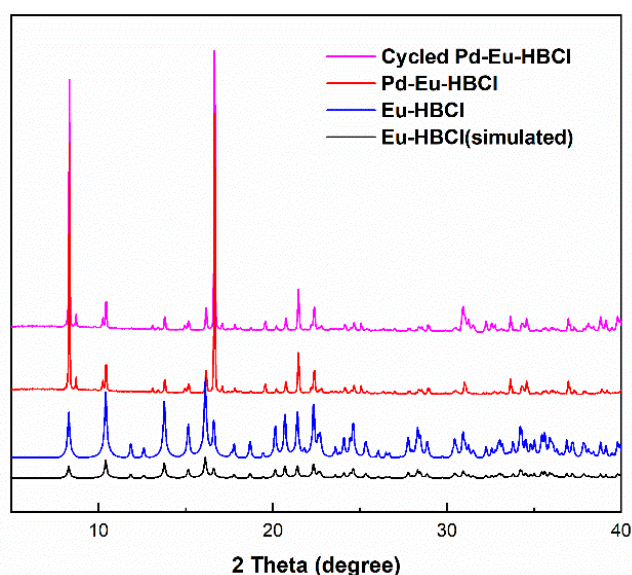


Figure 1. PXRD patterns of different samples.

In addition, thermogravimetric analyses (TGA) of Eu-BCI and Pd-NHC@Eu-BCI were carried out under N_2 atmosphere (Figure 2). The Eu-BCI initial total weight loss of 3.8% corresponding to the loss of the coordinated water molecule (calculated value: 3.7%) occurred at a temperature range of 150–250 °C. Above 300 °C, the framework structure began to collapse. Compared with Eu-BCI, the catalyst Pd-NHC@Eu-BCI had less weight loss. The reason for this phenomenon is that the lattice water molecules were partially removed during the PSM process. The TGA curves of Pd-NHC@Eu-BCI and the as-

synthesized Eu-BCI were almost the same, indicating that the modified 2D coordination polymer and catalyst had better stability.

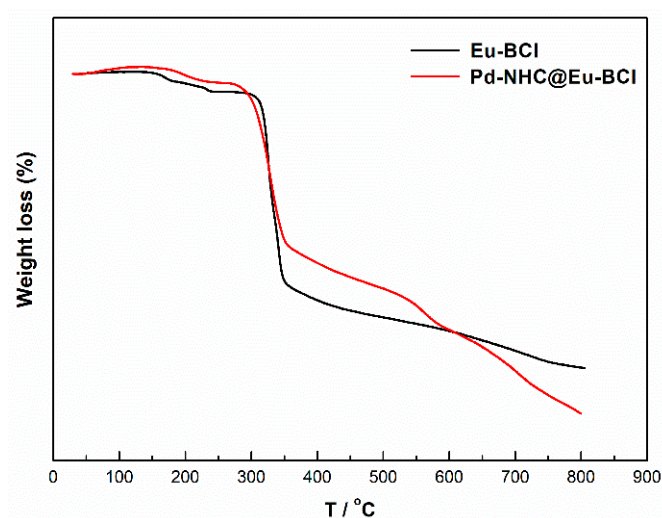


Figure 2. TGA plots of Eu-BCI and Pd-NHC@Eu-BCI.

The elemental composition of the catalyst was also analyzed by energy-dispersive X-ray spectroscopy (EDS). The EDS results confirmed the presence of C, N, O, Eu and Pd elements in the Pd-NHC@Eu-BCI (Figure S4). A scanning electron microscopy (SEM) image shows that the catalyst was composed of irregular blocks with a size of about 2–20 μm (Figure 3a). As observed in the transmission electron microscope (TEM) image, there were no Pd nanoparticles (Figure S5). Furthermore, the elemental mapping images show a homogeneous dispersion of Pd, Eu, O, and N elements, which also illustrate the successful synthesis of Pd-NHC@Eu-BCI (Figure 3b–e).

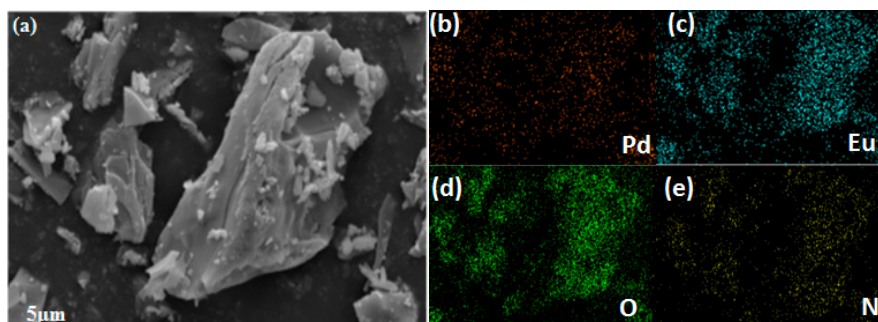


Figure 3. SEM (a) and the corresponding elemental mapping images of Pd-NHC@Eu-BCI (b–e).

The successful preparation of Pd-NHC@Eu-BCI was also confirmed by X-ray photoelectron spectroscopy (XPS), as shown in Figure 4. The XPS spectra revealed that all Pd species within the catalyst were in the divalent oxidation state [46,47], corresponding to the binding energies of 337.6 and 342.1 eV of Pd 3d_{5/2} and 3d_{3/2}, respectively (Figure 4b), which are also consistent with the values reported for Pd(II)-NHC complexes [48,49]. No peaks around 335 and 340 eV of the 3d_{5/2} and 3d_{3/2} levels of Pd(0) were observed [50,51], which confirms that there were no traces of Pd nanoparticles in the catalyst. On the other hand, no peaks of the binding energy of Pd(OAc)₂ were identified [52]. The N_{1s} XPS of Pd-NHC@Eu-BCI and Eu-BCI were measured. As shown in Figure 4c,d, the N_{1s} 398.2 eV binding energy peak of Eu-BCI was reduced, and the new peak of Pd-NHC@Eu-BCI N_{1s} formed near 400.2 eV, which is consistent with the peak of carbene-based compounds reported in the literature [53,54].

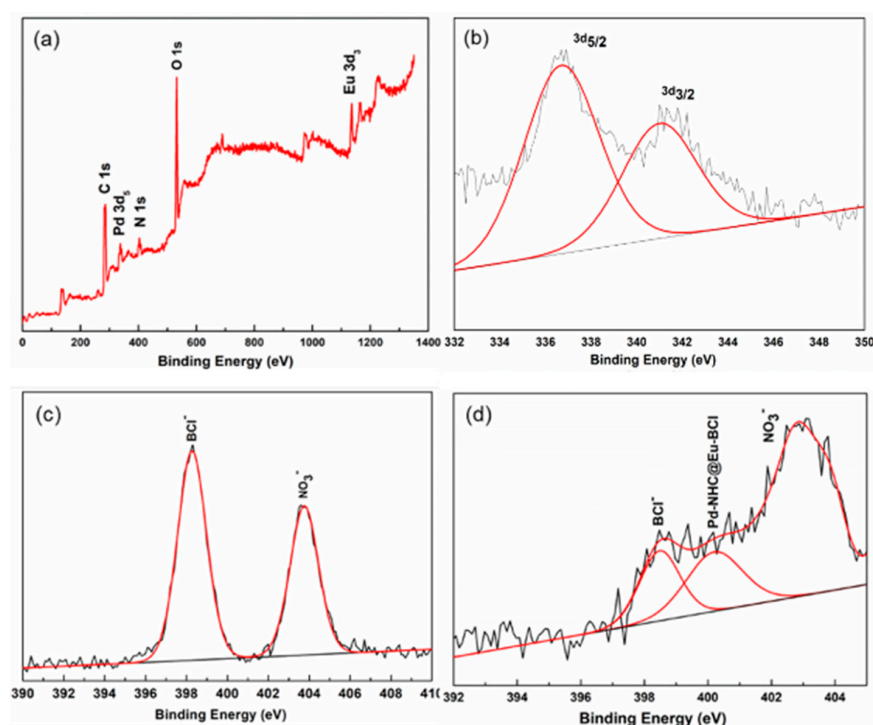
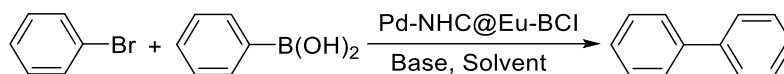


Figure 4. (a) XPS spectrum of Pd-NHC@Eu-BCI. (b) The Pd 3d XPS spectra of Pd-NHC@Eu-BCI. (c) The N 1s spectra of Eu-BCI. (d) The N_{1s} spectra of Pd-NHC@Eu-BCI.

3.2. Catalytic Activity

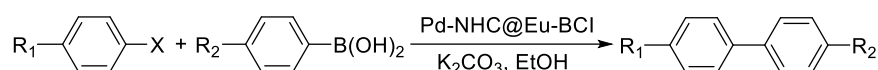
The C-C cross-coupling reaction of bromobenzene with phenylboronic acid was chosen as a model for the optimization of reaction conditions. The effect of different reaction parameters such as solvent, base, reaction time, catalyst amount and temperature were evaluated. First, different solvents such as DMF, toluene, H₂O and C₂H₅OH were used to find the best reaction media, in which the C₂H₅OH was the best solvent (Table 1, Entries 1–4). Several bases were applied and K₂CO₃ was the best choice (Table 1, Entry 4). When Cs₂CO₃, Et₃N or t-BuONa were used as alternative bases (Table 1, Entries 5–7), the yields decreased significantly. Next, we examined the catalyst amount (15 mg, 20 mg and 25 mg) and the results showed that 25 mg was the best amount. (Table 1, Entries 4, 11–12). Moreover, the reaction temperature of 80 °C was found to be optimal for the reactions (Table 1, Entries 4, 8–10). Thus, the optimum conditions selected were: K₂CO₃ as the base, C₂H₅OH as the solvent, 25 mg Pd-NHC@Eu-BCI at 80 °C with the yield 99%, corresponding to a turnover number (TON) of 374 and turnover frequency (TOF) of 62.3 h⁻¹. When Pd(OAc)₂ was used under the optimization of the reaction conditions, the yield of biphenyl was 87%. No significant catalytic activity was found when HBCl, Eu-BCI and Eu(NO₃)₃ were used in the couplings (Table S1).

To investigate the generality of Pd-NHC@Eu-BCI, substrates with various substituents were applied for the Suzuki–Miyaura coupling reaction under optimized reaction conditions (Table 2). Bromine and iodine derivatives could be reacted with phenylboronic acid to obtain good yields (Table 2, Entries 1–3). However, the yield was very low when chloride derivatives were used as substrates (Table 2, Entry 6). In addition, the electron-donating substituent (4-Me) substituted phenylboronic acid (Table 2, Entry 5) and the electron-withdrawing substituent (4-COMe) (Table 2, Entry 4) were studied. The experimental results showed that the yield of the former (4-Me, >99%) was higher than that of the latter (4-COMe, 92%), indicating that the catalyst was more inclined to catalyze the reaction of phenylboronic acid with an electron-donating substituent.

Table 1. Optimization of the reaction conditions for Suzuki–Miyaura coupling of bromobenzene with phenylboronic acid catalyzed by Pd-NHC@Eu-BCI.

Entry	Solvent	Base	Time (h)	Catalyst (mg)	Temperature (°C)	Yield (%)
1	DMF	K ₂ CO ₃	6	25	80	36
2	Toluene	K ₂ CO ₃	6	25	80	21
3	H ₂ O	K ₂ CO ₃	6	25	80	76
4	EtOH	K ₂ CO ₃	6	25	80	>99
5	EtOH	Cs ₂ CO ₃	6	25	80	64
6	EtOH	Et ₃ N	6	25	80	71
7	EtOH	t-BuONa	6	25	80	59
8	EtOH	K ₂ CO ₃	6	25	70	72
9	EtOH	K ₂ CO ₃	6	25	60	40
10	EtOH	K ₂ CO ₃	6	25	50	21
11	EtOH	K ₂ CO ₃	6	20	80	82
12	EtOH	K ₂ CO ₃	6	15	80	63

Reaction conditions: bromobenzene (1.0 mmol), phenylboronic acid (1.2 mmol), base (2.0 mmol), solvent (5.0 mL).

Table 2. Suzuki–Miyaura coupling reactions of aryl halides and arylboronic acids catalyzed by Pd-NHC@Eu-BCI.

Entry	Halide (R ₁ /X)	Arylboronic Acid (R ₂)	Yield (%)
1	H/I	H	99
2	CH ₃ /Br	H	99
3	COCH ₃ /Br	H	91
4	H/Br	COCH ₃	92
5	H/Br	CH ₃	99
6	COCH ₃ /Cl	H	31

Reaction conditions: aryl halide (1.0 mmol), arylboronic acid (1.2 mmol), K₂CO₃ (2.0 mmol), EtOH (5 mL), catalyst (25 mg), temperature (80 °C), time (6 h).

The proposed reaction mechanism of the Suzuki–Miyaura coupling reaction catalyzed by Pd-NHC@Eu-BCI is shown in Figure S6. First, the palladium catalytic cycle involves the oxidative addition of Pd(0) to the aryl halide to form an aryl palladium(II) complex. Then the aryl palladium(II) undergoes transmetalation with the arylboronic acid after complexation with the base. Finally, the biaryl product and re-establishment of the Pd(0) complex are generated in the reductive elimination step.

The heterogeneous nature of the catalyst was verified by the hot filtration test [55], which was carried out in the Suzuki–Miyaura cross-coupling reaction of bromobenzene with phenylboronic acid. The yield was 52% when Pd-NHC@Eu-BCI was removed by filtration after 3 h. No further conversion took place in the additional standing for 6 h of the filtrate (Figure 5), indicating the absence of a catalyst in the filtrate. On the other hand, the Pd and Eu contents in the biphenyl were tested by the ICP-AES after the reaction of bromobenzene with phenylboronic acid, which showed that no Pd or Eu was found in the coupling product.

As shown in Figure S7, Pd-NHC@Eu-BCI exhibited good reusability in the Suzuki–Miyaura reaction. The recovered catalyst was used for further reactions and showed consistent activity for at least four consecutive cycles (Figure 6), and the yield was significantly reduced in the fifth cycle. The morphology of the catalyst was maintained after being utilized in the Suzuki–Miyaura reaction by the SEM result. In addition, the PXRD (Figure 1) and XPS data (Figure S8) of the cycled Pd-NHC@Eu-BCI confirmed that the catalyst structure was essentially preserved during the reaction.

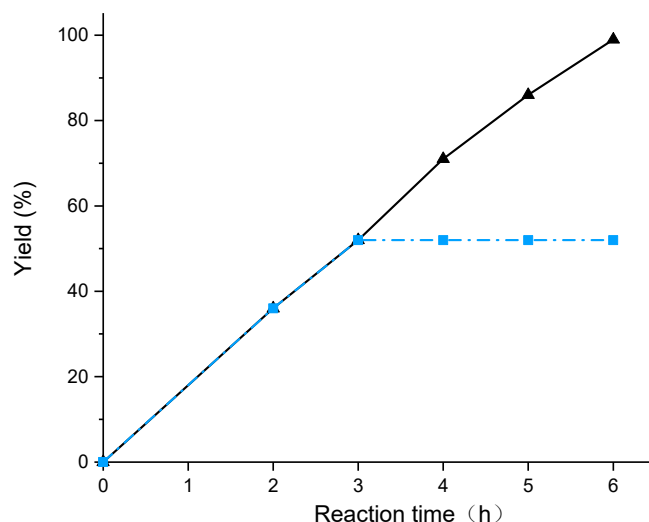


Figure 5. Time-dependent yields of the Suzuki–Miyaura cross-coupling reaction of bromobenzene with phenylboronic acid in the presence of Pd-NHC@Eu-BCI (solid line) or removal of Pd-NHC@Eu-BCI by filtration after 3 h reaction time (dashed line).

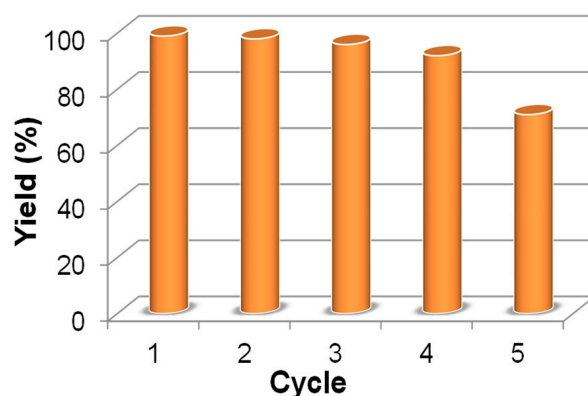


Figure 6. Recycling of Pd-NHC@Eu-BCI for Suzuki–Miyaura coupling reactions. Reaction conditions: bromobenzene (1.0 mmol), phenylboronic acid (1.2 mmol), K_2CO_3 (2.0 mmol), ethanol (5 mL), temperature (80 °C).

4. Conclusions

In summary, a two-step method was employed to construct a novel N-heterocyclic carbene–palladium heterogeneous catalyst Pd-NHC@Eu-BCI via a simple PSM process, by using the 2D coordination polymer Eu-BCI as the scaffold. The catalyst exhibits higher catalytic activity for the Suzuki–Miyaura coupling reaction. Moreover, Pd-NHC@Eu-BCI can be recycled and reused four times without a significant decrease in catalytic activity.

Supplementary Materials: The following supporting information can be downloaded at: <https://www.mdpi.com/article/10.3390/cryst13020341/s1>, Figure S1. The IR spectrum of Eu-BCI; Figure S2. The IR spectrum of Pd-NHC@Eu-BCI; Figure S3. (a) Coordination environment of Eu(III) in Eu-BCI. (b) View of 2D layer of Eu-BCI; Figure S4. EDS spectrum of Pd-NHC@Eu-BCI; Figure S5. TEM of Pd-NHC@Eu-BCI; Figure S6. The proposed reaction mechanism of Suzuki–Miyaura cross-coupling catalyzed by Pd-NHC@Eu-BCI; Figure S7. The SEM of Pd-NHC@Eu-BCI after five cycles; Figure S8. The Pd 3d XPS spectra of Eu-BCI- Pd after five cycles. Table S1. Suzuki–Miyaura coupling of bromobenzene with phenylboronic acid catalyzed by different samples.

Author Contributions: Conceptualization, L.Y. and Y.S.; investigation, R.T., X.W., J.H., S.X. and G.X.; writing—original draft, R.T., X.W., A.S.P. and L.Y.; resources, F.D. and Y.S.; funding acquisition, L.Y. and Y.S. All authors have read and agreed to the published version of the manuscript.

Funding: This work was supported by the Scientific Research Project from the Educational Department of Liaoning Province (LJKZ0432), the National Natural Science Foundation of China (21671139) and the National Key Research and Development Program of China (2020YFC1909300).

Institutional Review Board Statement: Not applicable.

Informed Consent Statement: Not applicable.

Conflicts of Interest: The authors declare no conflict of interest.

References

1. Guo, J.; Yao, S.X.; You, L.X.; Xiong, G.; Dragutan, I.; Dragutan, V.; Ding, F.; Sun, Y.G. Pd and Ni NPs@Eu-MOF, an economically advantageous nanocatalyst for C(sp²)-C(sp²) cross-coupling reactions. Key role of Ni and of the metal nanoparticles. *Polyhedron* **2022**, *223*, 115950. [[CrossRef](#)]
2. Veisi, H.; Zohrabi, A.; Kamangar, S.A.; Karmakar, B.; Saremi, S.G.; Varmira, K.; Hamelian, M. Green synthesis of Pd/Fe₃O₄ nanoparticles using Chamomile extract as highly active and recyclable catalyst for Suzuki coupling reaction. *J. Organomet. Chem.* **2021**, *951*, 122005. [[CrossRef](#)]
3. Baran, A.; Babkova, M.; Petkus, J.; Shubin, K. Suzuki–Miyaura arylation of 2,3-, 2,4-, 2,5-, and 3,4-dibromothiophenes. *Appl. Organomet. Chem.* **2022**, *36*, e6653. [[CrossRef](#)]
4. Bobers, J.; Hahn, L.K.; Averbeck, T.; Brunschweiger, A.; Kockmann, N. Reaction optimization of a Suzuki–Miyaura cross-coupling using design of experiments. *Chem. Ing. Tech.* **2022**, *94*, 780–785. [[CrossRef](#)]
5. Chen, X.; Wei, Z.; Huang, K.-H.; Uehling, M.; Wlekinski, M.; Krska, S.; Makarov, A.A.; Nowak, T.; Cooks, R.G. Pd reaction intermediates in Suzuki–Miyaura cross-coupling characterized by mass spectrometry. *ChemPlusChem* **2022**, *87*, e202100545. [[CrossRef](#)]
6. Gruß, H.; Feiner, R.C.; Mseyá, R.; Schröder, D.C.; Jewgiński, M.; Müller, K.M.; Latajka, R.; Marion, A.; Sewald, N. Peptide stapling by late-stage Suzuki–Miyaura cross-coupling. *Beilstein J. Org. Chem.* **2022**, *18*, 1–12. [[CrossRef](#)]
7. LaPorte, A.J.; Shi, Y.; Hein, J.E.; Burke, M.D. Stereospecific Csp³ Suzuki–Miyaura cross-coupling that evades β-oxygen elimination. *ACS Catal.* **2022**, *12*, 10905–10912. [[CrossRef](#)]
8. Lutfor Rahman, M.; Sani Sarjadi, M.; Salim Akhter, M.; Hannan, J.J.; Sarkar, S.M. Silica-coated magnetic palladium nanocatalyst for Suzuki–Miyaura cross-coupling. *Arab. J. Chem.* **2022**, *15*, 103983. [[CrossRef](#)]
9. Gao, M.Y.; Wang, J.M.; Shang, W.X.; Cai, Y.C.; Dai, W.L.; Wang, G.J.; Guan, N.J.; Li, L.D. Zeolite-encaged palladium catalysts for heterogeneous Suzuki–Miyaura cross-coupling reactions. *Catal. Today* **2023**, *410*, 237–246. [[CrossRef](#)]
10. Pearce-Higgins, R.; Hogenhout, L.N.; Docherty, P.J.; Whalley, D.M.; Chuentragool, P.; Lee, N.; Lam, N.Y.S.; McGuire, T.M.; Valette, D.; Phipps, R.J. An enantioselective Suzuki–Miyaura coupling to form axially chiral biphenols. *J. Am. Chem. Soc.* **2022**, *144*, 15026–15032. [[CrossRef](#)]
11. Ravbar, M.; Koler, A.; Paljevac, M.; Krajnc, P.; Kolar, M.; Iskra, J. Reusable Pd-polyHIPE for Suzuki–Miyaura coupling. *ACS Omega* **2022**, *7*, 12610–12616. [[CrossRef](#)] [[PubMed](#)]
12. Liang, Q.; Song, D. Iron N-heterocyclic carbene complexes in homogeneous catalysis. *Chem. Soc. Rev.* **2020**, *49*, 1209–1232. [[CrossRef](#)] [[PubMed](#)]
13. Sau, S.C.; Hota, P.K.; Mandal, S.K.; Soleilhavoup, M.; Bertrand, G. Stable abnormal N-heterocyclic carbenes and their applications. *Chem. Soc. Rev.* **2020**, *49*, 1233–1252. [[CrossRef](#)]
14. Mora, M.; Gimeno, M.C.; Visbal, R. Recent advances in gold-NHC complexes with biological properties. *Chem. Soc. Rev.* **2019**, *48*, 447–462. [[CrossRef](#)]
15. Tsang, W.C.; Munday, R.H.; Brasche, G.; Zheng, N.; Buchwald, S.L. Palladium-catalyzed method for the synthesis of carbazoles via tandem C-H functionalization and C-N bond formation. *J. Org. Chem.* **2008**, *73*, 7603–7610. [[CrossRef](#)] [[PubMed](#)]
16. Lakshman, M.K. Synthesis of biologically important nucleoside analogs by palladium-catalyzed C-N bond-formation. *Curr. Org. Synth.* **2005**, *2*, 83–112. [[CrossRef](#)]
17. Zhang, X.; Jiang, Y.; Fei, H. UiO-type metal-organic frameworks with NHC or metal-NHC functionalities for N-methylation using CO₂ as the carbon source. *Chem. Commun.* **2019**, *55*, 11928–11931. [[CrossRef](#)]
18. Qin, L.; Ji, Y.; Ding, T.; Liu, B.; Wang, R.; Ji, L.; Gao, G. Poly(ionic liquid)s-supported N-heterocyclic carbene silver complexes for the cycloaddition of CO₂ with epoxides. *Catal. Lett.* **2020**, *150*, 1196–1203. [[CrossRef](#)]
19. Renom-Carrasco, M.; Mania, P.; Sayah, R.; Veyre, L.; Occhipinti, G.; Gajan, D.; Lesage, A.; Jensen, V.R.; Thieuleux, C. Supported Ru olefin metathesis catalysts via a thiolate tether. *Dalton Trans.* **2019**, *48*, 2886–2890. [[CrossRef](#)]
20. Kamal, F.; Colombel-Rouen, S.; Dumas, A.; Guegan, J.P.; Roisnel, T.; Dorcet, V.; Basle, O.; Rouen, M.; Mauduit, M. Activation of olefin metathesis complexes containing unsymmetrical unsaturated N-heterocyclic carbenes by copper and gold transmetalation. *Chem. Commun.* **2019**, *55*, 11583–11586. [[CrossRef](#)]
21. Corma, A.; Serna, P.; Concepción, P.; Calvino, J.J. Transforming nonselective into chemoselective metal catalysts for the hydrogenation of substituted nitroaromatics. *J. Am. Chem. Soc.* **2008**, *130*, 8748–8753. [[CrossRef](#)] [[PubMed](#)]

22. Almallah, H.; Brenner, E.; Matt, D.; Harrowfield, J.; Jahjah, M.; Hijazi, A. Palladium complexes of N-heterocyclic carbenes displaying an unsymmetrical N-alkylfluorenyl/N'-aryl substitution pattern and their behaviour in Suzuki-Miyaura cross coupling. *Dalton Trans.* **2019**, *48*, 14516–14529. [[CrossRef](#)] [[PubMed](#)]
23. Qi, X.; Sun, H.; Li, X.; Fuhr, O.; Fenske, D. Synthesis and catalytic activity of N-heterocyclic silylene (NHSi) cobalt hydride for Kumada coupling reactions. *Dalton Trans.* **2018**, *47*, 2581–2588. [[CrossRef](#)] [[PubMed](#)]
24. Zhong, R.; Pöthig, A.; Feng, Y.; Riener, K.; Herrmann, W.A.; Kühn, F.E. Facile-prepared sulfonated water-soluble PEPPSI-Pd-NHC catalysts for aerobic aqueous Suzuki–Miyaura cross-coupling reactions. *Green Chem.* **2014**, *16*, 4955–4962. [[CrossRef](#)]
25. O'Brien, C.J.; Kantchev, E.A.; Valente, C.; Hadei, N.; Chass, G.A.; Lough, A.; Hopkinson, A.C.; Organ, M.G. Easily prepared air- and moisture-stable Pd-NHC (NHC=N-heterocyclic carbene) complexes: A reliable, user-friendly, highly active palladium precatalyst for the Suzuki-Miyaura reaction. *Chem. Eur. J.* **2006**, *12*, 4743–4748. [[CrossRef](#)]
26. Wei, W.; Qin, Y.; Luo, M.; Xia, P.; Wong, M.S. Synthesis, Structure, and catalytic activity of palladium(II) complexes of new CNC pincer-type N-heterocyclic carbene ligands. *Organometallics* **2008**, *27*, 2268–2272. [[CrossRef](#)]
27. Peris, E.; Mata, J.; Loch, J.A.; Crabtree, R.H. A Pd complex of a tridentate pincer CNC bis-carbene ligand as a robust homogenous Heck catalyst. *Chem. Commun.* **2001**, *2*, 201–202. [[CrossRef](#)]
28. Organ, M.; Chass, G.; Fang, D.-C.; Hopkinson, A.; Valente, C. Pd-NHC(PEPPSI) complexes: Synthetic utility and computational studies into their reactivity. *Synthesis* **2008**, *17*, 2776–2797. [[CrossRef](#)]
29. Boztepe, C.; Künkül, A.; Yaşar, S.; Gürbüz, N. Heterogenization of homogeneous NHC-Pd-pyridine catalysts and investigation of their catalytic activities in Suzuki-Miyaura coupling reactions. *J. Org. Chem.* **2018**, *872*, 123–134. [[CrossRef](#)]
30. Wei, Y.L.; Li, Y.; Chen, Y.Q.; Dong, Y.; Yao, J.J.; Han, X.Y.; Dong, Y.B. Pd(II)-NHDC-functionalized UiO-67 type MOF for catalyzing Heck cross-coupling and intermolecular benzyne-benzyne-alkene insertion reactions. *Inorg. Chem.* **2018**, *57*, 4379–4386. [[CrossRef](#)]
31. Anastas, P.; Eghbali, N. Green chemistry: Principles and practice. *Chem. Soc. Rev.* **2010**, *39*, 301–312. [[CrossRef](#)] [[PubMed](#)]
32. Polshettiwar, V.; Luque, R.; Fihri, A.; Zhu, H.; Bouhrara, M.; Basset, J.-M. Magnetically recoverable nanocatalysts. *Chem. Rev.* **2011**, *111*, 3036–3075. [[CrossRef](#)] [[PubMed](#)]
33. Pahlevanneshan, Z.; Moghadam, M.; Mirkhani, V.; Tangestaninejad, S.; Mohammadpoor-Baltork, I.; Loghmani-Khouzani, H. A new N-heterocyclic carbene palladium complex immobilized on nano silica: An efficient and recyclable catalyst for Suzuki–Miyaura C-C coupling reaction. *J. Org. Chem.* **2016**, *809*, 31–37. [[CrossRef](#)]
34. Vishal, K.; Fahlman, B.D.; Sasidhar, B.S.; Patil, S.A.; Patil, S.A. Magnetic nanoparticle-supported N-heterocyclic carbene-palladium(II): A convenient, efficient and recyclable catalyst for Suzuki–Miyaura cross-coupling reactions. *Catal. Lett.* **2017**, *147*, 900–918. [[CrossRef](#)]
35. Matharu, A.S.; Ahmed, S.; Almonthery, B.; Macquarrie, D.J.; Lee, Y.-S.; Kim, Y. Starbon/high-amylose corn starch-supported N-heterocyclic carbene-iron(III) catalyst for conversion of fructose into 5-hydroxymethylfurfural. *ChemSusChem* **2018**, *11*, 716–725. [[CrossRef](#)] [[PubMed](#)]
36. Xu, S.; Song, K.; Li, T.; Tan, B. Palladium catalyst coordinated in knitting N-heterocyclic carbene porous polymers for efficient Suzuki–Miyaura coupling reactions. *J. Mater. Chem. A* **2015**, *3*, 1272–1278. [[CrossRef](#)]
37. Chen, J.; Li, K.; Chen, L.; Liu, R.; Huang, X.; Ye, D. Conversion of fructose into 5-hydroxymethylfurfural catalyzed by recyclable sulfonic acid-functionalized metal-organic frameworks. *Green Chem.* **2014**, *16*, 2490–2499. [[CrossRef](#)]
38. Zeng, M.H.; Yin, Z.; Tan, Y.X.; Zhang, W.X.; He, Y.P.; Kurmoo, M. Nanoporous cobalt(II) MOF exhibiting four magnetic ground states and changes in gas sorption upon post-synthetic modification. *J. Am. Chem. Soc.* **2014**, *136*, 4680–4688. [[CrossRef](#)]
39. Dragutan, V.; Dragutan, I.; Xiong, G.; You, L.X.; Sun, Y.G.; Ding, F. Recent developments on carbon-carbon cross-coupling reactions using rare-earth metals-derived coordination polymers as efficient and selective Pd catalytic systems. *Resour. Chem. Mater.* **2022**, *1*, 325–338. [[CrossRef](#)]
40. You, L.X.; Yao, S.X.; Zhao, B.B.; Xiong, G.; Dragutan, I.; Dragutan, V.; Liu, X.G.; Ding, F.; Sun, Y.G. Striking dual functionality of a novel Pd@Eu-MOF nanocatalyst in C(sp²)-C(sp²) bond-forming and CO₂ fixation reactions. *Dalton Trans.* **2020**, *49*, 6368–6376. [[CrossRef](#)]
41. You, L.X.; Cui, L.X.; Zhao, B.B.; Xiong, G.; Ding, F.; Ren, B.Y.; Shi, Z.L.; Dragutan, I.; Dragutan, V.; Sun, Y.G. Tailoring the structure, pH sensitivity and catalytic performance in Suzuki-Miyaura cross-couplings of Ln/Pd MOFs based on the 1,1'-di(p-carboxybenzyl)-2,2'-diimidazole linker. *Dalton Trans.* **2018**, *47*, 8755–8763. [[CrossRef](#)] [[PubMed](#)]
42. You, L.X.; Liu, H.J.; Cui, L.X.; Ding, F.; Xiong, G.; Wang, S.J.; Ren, B.Y.; Dragutan, I.; Dragutan, V.; Sun, Y.G. The synergistic effect of cobalt on a Pd/Co catalyzed Suzuki-Miyaura cross-coupling in water. *Dalton Trans.* **2016**, *45*, 18455–18458. [[CrossRef](#)] [[PubMed](#)]
43. You, L.X.; Zong, W.; Xiong, G.; Ding, F.; Wang, S.; Ren, B.; Dragutan, I.; Dragutan, V.; Sun, Y. Cooperative effects of lanthanides when associated with palladium in novel, 3D Pd/Ln coordination polymers. Sustainable applications as water-stable, heterogeneous catalysts in carbon-carbon cross-coupling reactions. *Appl. Catal. A Gen.* **2016**, *511*, 1–10. [[CrossRef](#)]
44. You, L.X.; Zhao, B.B.; Yao, S.X.; Xiong, G.; Dragutan, I.; Dragutan, V.; Ding, F.; Sun, Y.G. Engineering functional group decorated ZIFs to high-performance Pd@ZIF-92 nanocatalysts for C(sp²)-C(sp²) couplings in aqueous medium. *J. Catal.* **2020**, *392*, 80–87. [[CrossRef](#)]
45. You, L.X.; Hao, J.H.; Qi, D.; Xie, S.Y.; Wang, S.J.; Xiong, G.; Dragutan, I.; Dragutan, V.; Ding, F.; Sun, Y.G. Lanthanide coordination polymers containing 1,3-bis(carboxymethyl) imidazolium as organic ligand: Crystal structure and luminescent properties. *Inorg. Chim. Acta* **2019**, *497*, 119075. [[CrossRef](#)]

46. Huang, J.; Wang, W.; Li, H. Water–medium organic reactions catalyzed by active and reusable Pd/Y heterobimetal-organic framework. *ACS Catal.* **2013**, *3*, 1526–1536. [[CrossRef](#)]
47. Bai, C.; Jian, S.; Yao, X.; Li, Y. Carbonylative Sonogashira coupling of terminal alkynes with aryl iodides under atmospheric pressure of CO using Pd(ii)@MOF as the catalyst. *Catal. Sci. Technol.* **2014**, *4*, 3261–3267. [[CrossRef](#)]
48. Liu, G.; Hou, M.; Wu, T.; Jiang, T.; Fan, H.; Yang, G.; Han, B. Pd(II) immobilized on mesoporous silica by N-heterocyclic carbene ionic liquids and catalysis for hydrogenation. *Phys. Chem. Chem. Phys.* **2011**, *13*, 2062–2068. [[CrossRef](#)]
49. Mohammadi, E.; Movassagh, B. Synthesis of polystyrene-supported Pd(II)-NHC complex derived from theophylline as an efficient and reusable heterogeneous catalyst for the Heck–Matsuda cross-coupling reaction. *J. Mol. Catal. A Chem.* **2016**, *418–419*, 158–167. [[CrossRef](#)]
50. Zhang, D.X.; Liu, J.; Zhang, H.X.; Wen, T.; Zhang, J. A rational strategy to construct a neutral boron imidazolate framework with encapsulated small-size Au–Pd nanoparticles for catalysis. *Inorg. Chem.* **2015**, *54*, 6069–6071. [[CrossRef](#)]
51. Tsyru'nikov, P.G.; Afonassenko, T.N.; Koshcheev, S.V.; Boronin, A.I. State of palladium in palladium-aluminosilicate catalysts as studied by XPS and the catalytic activity of the catalysts in the deep oxidation of methane. *Kinet. Catal.* **2007**, *48*, 728–734. [[CrossRef](#)]
52. Kong, G.Q.; Ou, S.; Zou, C.; Wu, C.D. Assembly and post-modification of a metal-organic nanotube for highly efficient catalysis. *J. Am. Chem. Soc.* **2012**, *134*, 19851–19857. [[CrossRef](#)] [[PubMed](#)]
53. Lu, J.; Yang, J.-x.; Wang, J.; Lim, A.; Wang, S.; Loh, K.P. One-pot synthesis of fluorescent carbon nanoribbons, nanoparticles, and graphene by the exfoliation of graphite in ionic liquids. *ACS Nano* **2009**, *3*, 2367–2375. [[CrossRef](#)] [[PubMed](#)]
54. Kovac, B.; Ljubic, I.; Kivimaki, A.; Coreno, M.; Novak, I. The study of the electronic structure of some N-heterocyclic carbenes (NHCs) by variable energy photoelectron spectroscopy. *Phys. Chem. Chem. Phys.* **2015**, *17*, 10656–10667. [[CrossRef](#)]
55. Çalışkan, M.; Baran, T. Immobilized palladium nanoparticles on Schiff base functionalized ZnAl layered double hydroxide: A highly stable and retrievable heterogeneous nanocatalyst towards aryl halide cyanations. *Appl. Clay Sci.* **2022**, *219*, 106433. [[CrossRef](#)]

Disclaimer/Publisher's Note: The statements, opinions and data contained in all publications are solely those of the individual author(s) and contributor(s) and not of MDPI and/or the editor(s). MDPI and/or the editor(s) disclaim responsibility for any injury to people or property resulting from any ideas, methods, instructions or products referred to in the content.